# Automation of Bird Front Half Deboning Procedure: Design and Analysis

Debao Zhou, Jonathan Holmes, Wiley Holcombe, Kok-Meng Lee* and Gary McMurray
Food Processing Technology Division, ATAS Laboratory, Georgia Tech Research Institute,
*School of Mechanical Engineering, Georgia Institute of Technology,
Atlanta, GA 30332

**Abstract**—*Bio-material cutting, such as meat deboning, is one of the most common operations in the food processing industry. It is also the largest employer of people in the United States. These tasks are currently manual processes with only limited use of fixed automation. The main difficulty in this task is the natural variability of the product's size and individual anatomy. The industry is looking to robotics to help solve these problems. This research has focused on automating the cutting of chicken front halves to obtain high quality breast meat. In order to specify the cutting locations and cutting trajectories on chicken front halves, in this paper, the anatomy structure of the chicken shoulder joint was studied first. Then a 2-DOF cutting mechanism was proposed. Through the formulation of the kinematics and dynamics of the mechanism, the cutting trajectory was simulated. Pneumatic actuators with position feedback sensors were selected as the driven system. To verify whether the pneumatic driving system could satisfy the trajectory following requirements (speed and response time), experiments were carried out. The results show that the pneumatics driven system can marginally follow the desired trajectory with enough speed for the adaptation motion. The device will be built and tested in our future research.*

**Keywords: robotics, poultry deboning, pneumatic drives**

## I. Introduction

The procedure to manually harvest the chicken breast meat and wings (butterfly) is shown in Fig. 1. A front half is fixed on a cone as shown in Fig. 1(a). After the joint connections are severed, the wing and breast meat are separated from the carcass by pulling the butterfly (Fig. 1(b)) away from the carcass (Fig. 1(c)). The wing pulling motion is shown in Fig. 1(d), where *F* is the pulling force direction.

Considering this process has to be manually repeated approximately 300,000 of chickens each day, it is obviously very onerous. However, due to the naturally deformable bodies, size difference and possible hard bone chips in meat, it is very difficult to be automated. One commercial solution is the automation deboning lines by the Stork Gamco Inc. [1]. However, their method still belongs to the fixed automation category since they require the cutting motions be preset manually and thus, they cannot automatically adjust to changes in individual bird sizes. Meyn Inc. [2] also developed a cutting device. Their cutting device has only one fixed motion for all the front halves deboning. In order to adapt to the variations in chicken size, Delay *et al.* [3] proposed a reference-point method to estimate the locations of the cutting trajectory and these reference points were obtained through the analysis of the computer images. Using a similar method, Heck [4] proposed to use water-jet cutting method to cut chicken breast meat to obtain certain shapes according to the identified trajectory from computer images. Some research on deboning has also been carried out on the pork or beef deboning such as [5] and [6]. The pork and beef deboning in these works is to cut through everything including hard bones, while the deboning in chicken tries to avoid hard bones in order to obtain high quality butterfly.

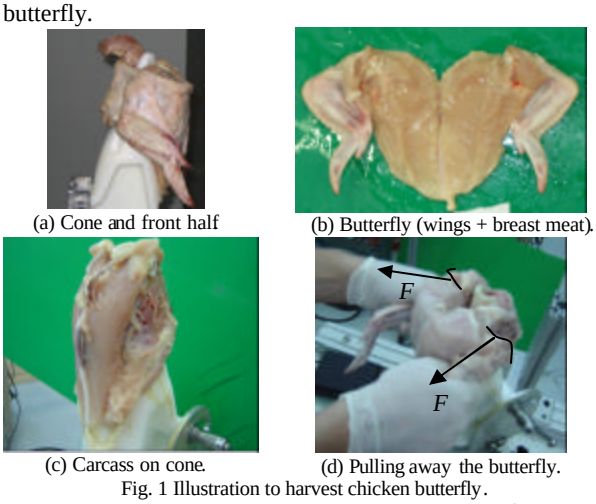


(a) Cone and front half (b) Butterfly (wings + breast meat).
(c) Carcass on cone. (d) Pulling away the butterfly.

Fig. 1 Illustration to harvest chicken butterfly.

Currently, no cutting device is available for this automation with the capability to adapt to the size-change and body-deformation. In this research, through the understanding of the anatomy of chicken shoulder joints, a new processing method associated with a simple mechanism was proposed. Note that the scope of this paper is to design a device which has the ability to adapt the bio-material deformation during deboning. The adaptability will be further studied through the motion control and force control.

In the following, the anatomy of the deboning related chicken body was studied and the cutting trajectories were specified in Section II. According to the front half transportation method in industry, the cutting system was specified and the simulated trajectory following motion using the cutting mechanism was shown in Sections III and IV. The driven device was selected and verified in Section V. After the discussion in Section VI, remarks were specified.

## II. Deboning Related Chicken Shoulder Anatomy

### *A. Chicken Shoulder Anatomy*

The deboning related components in a chicken body s include the front half skeleton and the connection anatomy between the wing and the carcass. Fig. 2 shows the skeleton of a chicken front half. Reference [7] has shown the detailed study. However, their anatomy study cannot be directly applied to the cutting device design.

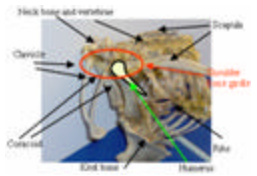

Fig. 2 Front half skeleton.

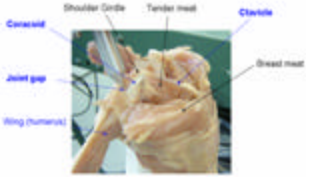

Fig. 3 Outside view.

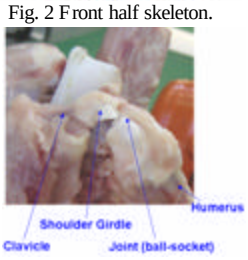


Fig. 4 Top ligament and meat.


Fig. 5 Humerus and ligaments.

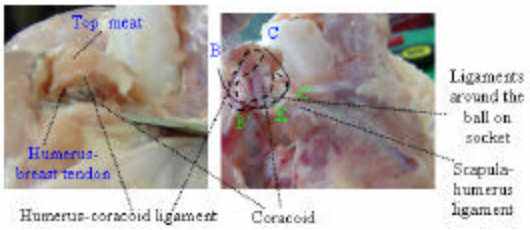


(a) Top view. (b) View from wing direction.

Fig. 6 Joint ligaments and tendon connection area.

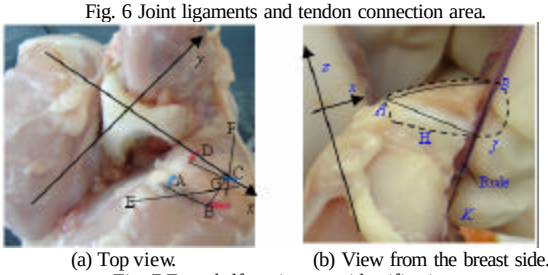

(a) Top view. (b) View from the breast side.

Fig. 7 Front half cutting area identification.

As shown in Fig. 2, the scapula, coracoid and clavicle bones form a shoulder bone girdle. The right and left girdles connect to the vertebrate through the ribs. The coracoids connect together through the keel bone. In fresh chickens, the wish bones (clavicles) connect with the keel bone through soft tissues. The location and orientation of the humerus and breast meat relative to the skeleton is shown in Fig. 3. The area below the breast meat and between the coracoid and humerus is the starting portion of the tender meat. A ball-socket joint is formed between the humerus and the carcass by the ligaments, tendons and meat. When a fresh chicken wing is pulled, a small gap (about 2 -5 mm) is formed between the humerus and the shoulder bone girdle. This gap provides the space for a blade to enter the joint through cutting the connecting ligaments. The gap increases when the top ligament is cut as shown in Fig. 4. There are 5 main ligaments/tendons connecting the humerus to the carcass as shown in Fig. 5. There are three ligaments connecting the humerus and the coracoid, one tendon connecting the breast meat with the humerus and one ligament connecting the scapula and humerus. These ligaments and tendons occupy about ¾ of a circle perimeter around the joint and leave about ¼ joint near the neck empty, as shown in Fig. 6(b).

The carcass and bone structure without the breast meat and wings are shown in Fig 7(b). The joint length from top is about 25mm. As shown in Fig. 7(a), the distance between ruler and clavicle is about 25mm and the thickness of the top meat (*BJ*) is about 5 mm. The angle between the ruler and the upward direction of the cone is about 17°. Note that for different size chickens, the above dimensions are different. The cutting device should have the ability to adjust to adapt to the variations.

### *B. Cutting Area and Cutting Trajectory*

A frame *oxyz* is defined on the chicken as shown in Fig. 7. The upward direction of the cone is the positive *z* axis. Two points are identified as reference points: in the z direction, the highest coracoid points on the left and right, where there is a small dent. The *x* axis is formed by connecting these two points. In Fig. 7, point *A* is the location where the clavicle connects to coracoid; *G* is the middle point of the joint gap; *BC* is the joint gap location; Ruler surface plane shown as *BK* in Fig. 7(b) or plane (BB'KC'C) in Fig. 6(b) is the joint cutting plane. The coracoid is under the area of *ABCD* as shown in Fig. 7(a).

In order to pull away the butterfly, the connections with area *ABCD* through lines *AB*, *BC* and *CD* need to be severed. Thus the 'must cut' areas are *BB'KC'C* in Fig. 6(b) and area *AHJB* in Fig. 7(b). The following parameters will change with chicken size: (1) length of *AB*, (2) length of *BC*, (3) shift distance of *ABJ* plane in the parallel direction to the *AB* position shown in Fig. 7(a) and (4) the shift distance of *BB'KC'C* plane in the parallel to the shown plane *BB'KC'C*. The 'must not cut' areas are as follows: (1) the area from *B* to *A* but not passing point *A* due to the clavicle bone, (2) from point *C* to *B* but not passing point *B* due to the protection of the breast meat, (3) area *ABCD* due to the coracoid, (4) *BC* to chicken wing due to the humerus. The 'can be cut' areas are as follows: (1) from *A* to *B*, but passing point *B*, (2) from *B* to *C* but passing point *C*, (3) region *CF* and (4) the region below *B'KC'*, where there is either empty/cone or scapula/coracoid. The cutting path from A to B to C can be a smooth curve (such as a circle) or straight lines *AB*, *BC*.

In this research, in order to simplify the cutting device, the planes *ABJ* and *BB'KC'C* are selected as the cutting

trajectory. The requirement for the size adaptation is to deal with the size, location and orientation change of the two planes.

## III. Deboning System and Cutting Device

It is assumed in this research that a front half is fixed on cone and the cone moves together with the conveyor at 10in/s. It is also assumed that the cone can provide all the required roll, yaw and pitch motions. The other requirements for the cutting device are the 'must cut' trajectory must be followed, 'must not cut" region cannot be entered, chicken size must be adapted and cutting force must be small enough to avoid damaging the carcass bone structure and to keep the deformation of the carcass very small.

Five deboning stations are used to harvest breast meat. The first one is the vision station which is used to identify the location of the chicken joint relative to the cone. The second is the scapula cut station. The next two are for the left and right clavicle cuts. The last one is for the joint cut. The cutting stations, cone, front halves and conveyor are shown in Fig. 8. The cutting device is shown in Fig. 9.

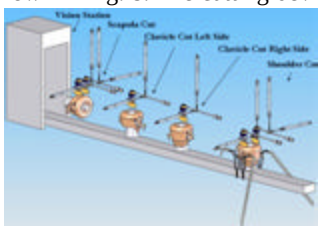

Fig. 8 Cutting system diagram.

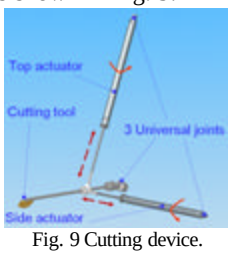


Fig. 9 Cutting device.

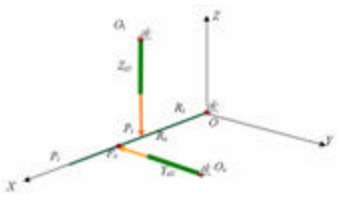

(a) Initial location.

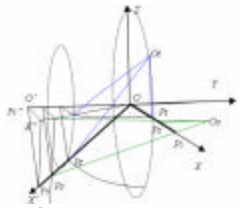

(b) One cutting posture.

Fig. 10 schematic illustration of the cutting device.

The current research focuses on building a prototype to test the cutting method instead of building the whole cutting system. Thus in the following, the cutting device in Fig. 9 is discussed only.

The cutting tool handle is fixed to the base through a universal joint. The handle connects with two linear actuators: top actuator and side actuator. The top actuator is mainly for cutting and the side actuator is mainly for chicken size adaptation. The other side of the actuators is also fixed to the base through a universal joint. The two actuators and the handle can rotate freely relative to its universal joint.

The handle is driven by the translation motion of the two cylinder pistons and its schematic diagram is shown in Fig. 10, where the frame *OXYZ* is fixed to eh base (a space-fixed frame).

In *OXYZ* frame, point $O_t(R_t, 0, Z_{t0})$ is the base location of the top actuator, $O_s(R_s, Y_{s0}, 0)$ is the base location of the side actuator, $P_t$ $(R_t, 0, 0)$ is the top actuator/handle connection point, $P_s$ $(R_s, 0, 0)$ is the side actuator/handle connection point and $P_i$ $(L, 0, 0)$ is the cutting trajectory in *OXYZ* frame. Parameters with subscript *t* are for the top cylinder and those with subscript *s* are for the side cylinder. The moving distance in *Y* direction is $d_y$ and in *Z* direction is $d_Z$, where $d_y$ is for the chicken size adjustment and $d_z$ is for the clearance adjustment and cutting motion. The initial position is at *OX* and the final position is at *OX'*, where the plane *O'P_i'P_i"* is parallel to *OXZ* plane, thus $d_y = |OO'|$ as shown in Fig. 10(b). The distance from point $P_i'$ to *XOY* plane is $d_Z$. The coordinate of point $P_i'$ is $(d_x, d_y, d_z)$, where $d_y < 0$, $d_z < 0$ and $L^2 = d_x^2 + d_y^2 + d_z^2$. So there is

$$\dot{d}_x = \left(\dot{d}_y d_y + \dot{d}_z d_z\right) / d_x .$$

The coordinate of $P_t'$ is $R_t/L(d_x, d_y, d_z)$. The vector $O_tP_t'$ is

$$\mathbf{r}_t = R_t/L[d_x, d_y, d_z]^T - [R_t, 0, Z_{t0}]^T,$$

where vector $\mathbf{r}$ express the piston end location in the *OXYZ* frame and

$$\dot{\mathbf{r}}_t = R_t\left[d_y\dot{d}_y / d_x + d_z\dot{d}_z / d_x, \dot{d}_y, \dot{d}_z\right]^T / L .$$

The coordinate of $P_s$ is $(d_x, d_y, d_z)R_s/L$. The vector $O_sP_s$ and its derivative with time are

$$\mathbf{r}_s = [d_x, d_y, d_z]^T R_s/L - [R_s, 0, Z_{s0}]^T,$$

$$\dot{\mathbf{r}}_s = R_s\left[d_y\dot{d}_y / d_x + d_z\dot{d}_z / d_x, \dot{d}_y, \dot{d}_z\right]^T / L .$$

Thus the motions of the two cylinders can be determined by predefined $d_y$, $d_z$. In size adaptation motion, $d_z = 0$. There are

$$L^2 = d_x^2 + d_y^2,$$

$$\dot{d}_x = \dot{d}_y d_y / d_x .$$

The coordinate of $P_t$ is $(d_x, d_y, 0)$ $R_t/L$. The vector $O_tP_t$ is

$$\mathbf{r}_t = R_t/L[d_x, d_y, 0]^T - [R_t, 0, Z_{t0}]^T.$$

So

$$\dot{\mathbf{r}}_t = R_t\left[d_y\dot{d}_y / d_x, \dot{d}_y, 0\right]^T / L .$$

The coordinate of $P_s$ is $(d_x, d_y, 0)$ $R_s/L$. The vector $O_sP_s$ and its derivative with time are

$$\mathbf{r}_s = R_s/L[d_x, d_y, 0] - [R_s, 0, Z_{s0}],$$

$$\dot{\mathbf{r}}_s = R_s\left[d_y\dot{d}_y / d_x, \dot{d}_y, 0\right] / L .$$

For the clearance of the adjustment and cutting motion, $d_y$ ? 0 and keeps constant ( $\dot{d}_y = 0$). There are

$$L^2 = d_x^2 + d_y^2 + d_z^2,$$

$$\dot{d}_x = \dot{d}_z d_z / d_x .$$

The coordinate of $P_t$ is $(d_x, d_y, d_z)$ $R_t/L$ and the vector $O_tP_t$ is

$$\mathbf{r}_t = R_t/L[d_x, d_y, d_z] - [R_t, 0, Z_{t0}],$$

and its time derivative is

$$\dot{\mathbf{r}}_t = R_t\left[d_z\dot{d}_z / d_x, 0, \dot{d}_z\right]^T / L .$$

The coordinate of $P_s$ is $(d_x, d_y, d_z)$ $R_s/L$ and the vector $O_sP_s$ and its derivative with time are

$$\mathbf{r}_s = R_s\,[d_x, d_y, d_z]^T / L - [R_s, 0, Z_{s0}]^T,$$

$$\dot{\mathbf{r}}_s = R_s\left[d_z\dot{d}_z / d_x, 0, \dot{d}_z\right]^T / L .$$

## IV. Cutting Trajectory Simulation

The important parameters in this research are the moving speed of the front halves, 10 in/s with 12 inch interval. For the *AB* and *BC* cut, the moving distance is about 1 inch. Thus the cutting takes about 100ms.

For *AB* cut, the blade plane (*OX'Z*) should lies in the *ABJ* plane as shown in Fig. 11. Note the orientation difference between the blade plane and its initial plane. It is assume that the two planes *OX'Z* and *OXZ* in Fig. 10(b) are in the same orientation (plane normal vectors are the same). The problems (yield drop and cutting position errors) brought by this assumption will be discussed later. The maximum breast meat cut depth in *AB* cut is less than 0.5 inch. If *BM* in positive *OX* direction is 1/4 inch and *BJ* is 0.5 inch in *OZ* direction, it takes 25ms. Note *Z* direction moving speed is 0 at point *J*, thus the moving trajectory in positive X direction is 1.5 inch (1 inch for height adjustment and 0.5 inch for cut depth). It is accelerated from the contact point between the blade and the meat and de-accelerated to 0 at the moving distance in -*Z* is 1.5inch.

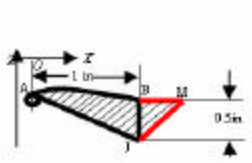


Fig. 11 *AB* cut trajectory.

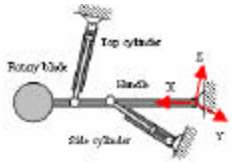


Fig. 12 *BC* cutting device.

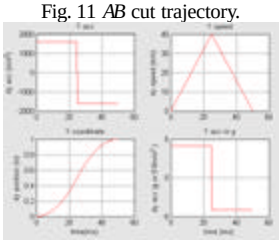

Fig. 13 Desired *Y* motion.

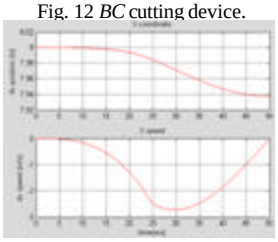

Fig. 14 Corresponding *X* motion.

For *BC* cut, the blade plane (*OX'Z*) should lie in the *BB'C'C* plane. The moving distance in *OZ* direction is about 1 inch and in *OX'* direction is about 1/4 inch. In order to realize slicing cut, rotary blade is used as shown in Fig. 12. Since moving 1 inch in *X* direction takes 100 ms, moving 1/4 inch in *X* direction takes about 25ms. At the same time, the *Z* direction moving distance is 1 inch. Thus the *Z*-direction average moving speed of the cutter is about 40 in/s from *B* to *B'* and from *C'* to *C*. At points *B'* and *C'*, the speed in *Z* direction is zero. The other simulation values are as follows: coordinate of $O_t$ as {4, 0, 4} inch, $O_s$ as {6, 4, 0} inch, *S* as 1 inch $S_z$ as 2 inch, *L* as 8 inch, moving time is 50ms and the acceleration is 1/2 of the whole moving time.

In size-adaptation motion, the knife moves in the *OXY* plane, thus $d_z = 0$ and the final value of $d_y$ is set as 1 inch. The desired motion in *OY* direction is shown in Fig. 13 and the corresponding motion in *OX* is shown in Fig. 14.

Since the motion in *Z* direction keeps at 0, only *Y* and *X* motions are shown. In Fig. 13, the *Y* coordinate changes 1 inch and the acceleration is about 5*g*, where *g* is gravity acceleration. Fig. 15 shows the cylinders' motion in order to generate the trajectories shown in Figs. 13 and 14. The top cylinder piston moves about 0.03 inch and the side cylinder piston moves about 0.8 inch. The maximum speed magnitude for the top cylinder is 20 inch/s and the side cylinder is about 30in/s.

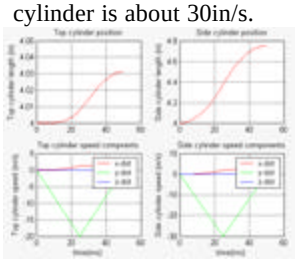

(a) Two pistons' motions

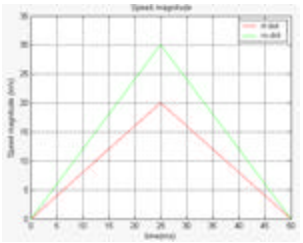

(b) Resultant speed of each piston

Fig. 15 cylinders' trajectory in AB adjustment cut motion

In cutting motion, $d_y$ keeps constant at 1 inch and $d_z$ changes from 0 to 2 inches. Since *BC* needs more moving distance in *Z* direction than *AB* cut, only *BC* cut is simulated for the cutting motion. The ratio between the acceleration and whole moving down motion is set as 1/2, which means that 1 inch is for acceleration of the blade in *Z* direction and 1 inch is for the joint cut (deceleration in *Z* direction). The *Z* motion trajectory is shown in Fig. 16. The corresponding *X* motion is shown in Fig. 17.

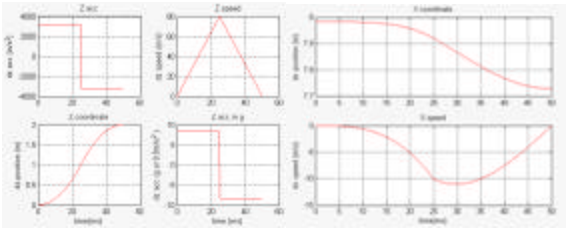

Fig. 16 *BC* cut, *Z* desired motion

Fig. 17 *BC* cut, *X* motion

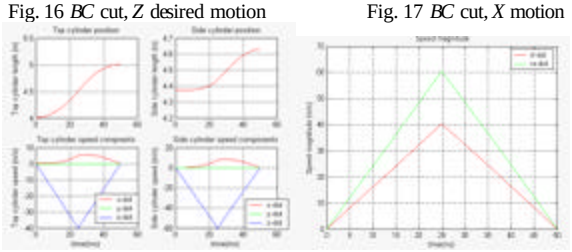

Fig. 18 Cylinders trajectory in BC cutting motion.

The acceleration for the blade is about 8*g* and moving distance is 2 inch in 50 second. The *X* motion is about 0.3 inch and about 12 in/s. In order to generate this motion, the cylinders' motion is shown in Fig. 18. From the results, it is observed that the moving distance of the top cylinder piston is about 1 inch and maximum speed is about 60 in/s, and 0.3 inch and 40 in/s for the side cylinder.

## V. Applicability Verification

From Section IV, it is seen that the blade needs to move 2 inches in 50ms. Thus the most critical requirements for the cylinder are extending 1 inch in 50s and extending 1/2 inch in 25s. The other location/time

relations are not critical. It is desired to use a pneumatic system to realize this motion due to its price and mechanical simplicity. The Enfield LS-V15 valve, LS-C10 controller, and Numatics ACC M series cylinder 15AM 1-06A [8] were used for the verification. The experimental device and the system connection diagram are shown in Fig. 19 (a) and (b), respectively.

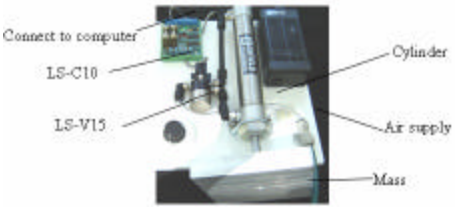


(a) Experimental device.

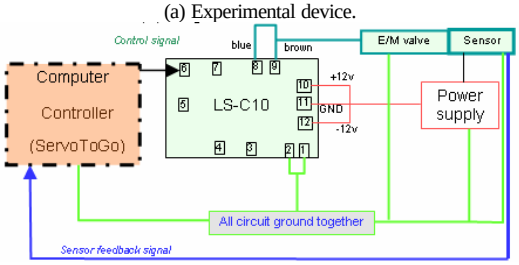


(b) Connection diagram.

Fig. 19 Experimental device and connection diagram.

The relationship between the feedback volt age and the actual piston position of the system was calibrated first and the results are shown in Fig. 20. By adjusting difference gains, the step response is obtained as shown in Fig. 21. It is observed that when control gains are P gain ($K_p$) = 1950 and D gain ($K_d$) = 300, the best control results are obtained.

When the valve is fully opened, the maximum acceleration can be reached. High voltage is provided to the LS-C10 controller to make sure the LS-V15 valve is fully opened. The piston position, speed and acceleration versus time, respectively, are shown in Fig. 22. It is observed that the maximum speed is 55 in/s and the average speed is 23 in/s.

In these experiments, the commanded moving distance was a step signal with 1 inch in magnitude. The open status of the valve was recorded in the experiments to show the possibility to change to a bigger valve. The experimental results are shown in Fig. 23.

It is seen from Fig. 23 that the valve is fully opened for the initial command of the position change. It took about 40s for piston to reach commanded position (1 inch). Further experiments showed that if it is fully opened, the response time was about 33ms to 50 ms with 60% overshoot. When more load mass was added to the piston, it was observed that the system was capable to drive to the 1 inch position in 50 ms. The results for the 1 inch step response with and without mass are shown in Fig. 24. The time delay is observed when more mass is added.

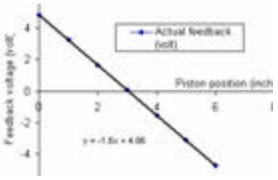


Fig. 20 Piston position feedback and actual piston position.

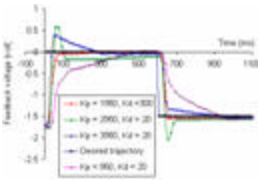

Fig. 21 Step response to different control gains.

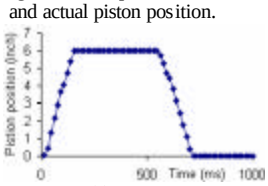


(a) Piston position.

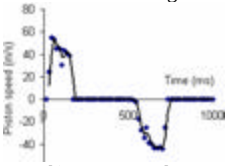


(b) Piston speed.

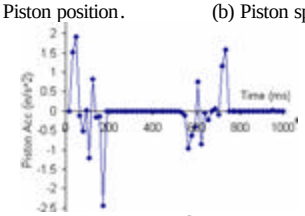


(c) Piston acceleration.

Fig. 22 Piston motion characters when valve is fully opened

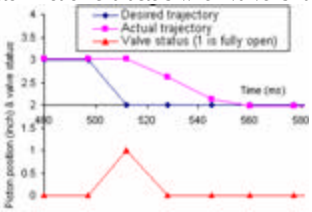


Fig. 23 Response to a step input with valve status.

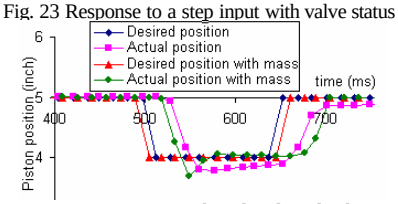


Fig. 24 Step response with and without load mass.

## VI. Discussions

### *A. Response Time*

Response time is often defined as the interval from the instant when a user initiates a request to the instant at which the first part of the response is received. In this study, the response time is defined as the interval from the moment when the command signal (step signal) is sent out to the moment when the response of the piston position reaches 95% of the command signal. In these experiments, it was observed that when the commanded step trajectory was 1 inch, the response time was about 35ms to 50ms. In the desired trajectory, when the moving distance is about 1 inch, the response time is about 50ms. The maximum speed is about 55 in/s, but the desired maximum speed is 60 in/s. It can be predicted that at 25ms, the piston cannot reach the 0.5in location.

The response time mainly depends on the following parameters: (i) the magnitude of the signal, (ii) the control

gain (i. e. valve open area, or mass flow rate), (iii) compression air pressure, (iv) the friction force on the piston and (v) the inertia of the piston and load. With larger load mass, the response time will be longer. In the experiments, the load mass is 2.35 lb. The maximum acceleration can be realized when (a) the valve is fully opened and/or (b) the maximum pressure is realized without fully open the valve. Two methods can be use to increase this maximum speed to 60 in/s by either using to a bigger valve or changing to a smaller inner diameter cylinder. Using a bigger valve generates bigger overshoot. The sampling time of the current control system is about 13 ms and the sampling frequency is obviously too slow. Using a shorter sampling time control system, the control results may be better in the sense of faster and smooth response and lower overshoot.

It can be seen that the tested pneumatic system can marginally satisfy the design requirements.

*B. Orientation Error Analysis*

In the simulation, $d_y$ was set as 1 inch. For *AB* and *BC* cut, by selecting a middle position of the chicken size, the value can be set as $d_y = \pm 0.5$ inch. If the blade handle length is 8 inch, the angle to *OXZ* plane satisfy $d = 3.58°$. Suppose the vision system can provide very good results to make the plane *ABJ* and *BB'KC'C* are parallel with the moving direction and in the *OXZ* plane, it can be seen that the angle between the blade side plane and cutting plane is 3.58°. Suppose the *AB* or *BC* cutting trajectory is 1 inch, the error generated in *OY* direction is $\Delta y = 0.0625$ inch. For *AB* cut, due to this misalignment, the meat chunk in this regain is less than 5 mm in thickness. The meat due to this error is very small when compared to whole breast meat. For the *BC* cut, the joint gap can be 2-5mm. If the blade knife intercepts with *BB'KC'C* and the middle of *BC*, due to the round shape of the ball part of the humerus, the influence of this error can be definitely ignored. This will be further verified using our final mechanism.

## VII. Conclusions

The food processing industry is very dependent on manual labor due to the diverse set of tasks that must be performed on a product that has no consistent physical parameters. This research work was focused on the development of an intelligent cutting system capable of using robotics to automatically adapt to variations in bird size and anatomy. The following conclusions were drawn:

(i) The deboning related anatomy of chicken front halves was described in detail. Simple cutting trajectories were identified. This work results in the selection of the cutting trajectories with simple motion.

(ii) The cutting system was proposed and a simple cutting device capable of size adaptation was designed.

(iii) The kinematics of the cutting device formulated and the cutting trajectory was simulated using identified parameters and the cutting mechanism.

(iv) The pneumatic driven system with position feedback was identified. The experimental results showed that this driven system can marginally satisfy the design requirements of the cutting motion.

Based on this preliminary work, the research team will build the dynamic model of the pneumatic driven system to further verify this mechanism. This prototype, once it is built, will be tested on a bird shoulder deboning.

## Acknowledgement

This project is supported by the State of Georgia through the Agriculture Technology Research Program at the Georgia Tech Research Institute. The team would also like to thank Enfield Inc. for providing the experimental pneumatic device.

## References

[1] Stork Gamco Inc, *http://stork.com/gamco/page.html?id=7610*, Jan. 2007.

[2] Meyn Food Processing Technology B.V., *http://www.meyn.nl /index.php?option=com_content&task=view&id=123&Itemid=34*, Jan. 2007.

[3] Daley, W., He, T. Lee K-M; Sandlin, M., Modeling of the natural product deboning process using biological and human models, in the *Proceedings of 1999 IEEE/ASME International Conference on Advanced Intelligent Mechatronics*, pp: 49 – 54, Sept. 19-23, 1999.

[4] Heck, B., Automated chicken processing: machine vision and water-jet cutting for optimized performance, *IEEE Control Systems Magazine*, 26(3) 17-19, June 2006.

[5] Dempsey P. G. and McGorry R. W., Investigation of a pork shoulder deboning operation, *Journal of Occupational and Environmental Hygiene*, vol 1, pp. 167-172, 2004.

[6] McGorry R. W., Dowd P. C. and Dempsey P. G., The effect of blade finish and blade edge angle on forces used in meat cutting operations, *Applied Ergonomics*, Elsevier publications, vol. 35, pp. 71-77, 2005.

[7] Chamberlain, F. *Atlas of Avian Anatomy.* Michigan State College, Agricultural Experiment Station, East Lansing, MI. Hallenbeck Printing Company, Lansing, MI, 1943.

[8] Numatics Actuator Group, *Accu M Series Position Feedback Actuators*, ACCUMCAD, Feb. 2006.